



www.elsevier.com/locate/jvc

Case Report

Histological evidence of myxomatous tissue in a Labrador puppy with pulmonic stenosis and tricuspid valve dysplasia[★]



J. Schoebel a,b,*, G. Wess a, M. Tursi c

- ^a Small Animal Clinic, Ludwig-Maximilians University, Veterinaerstr. 13, 80539, Munich, Germany
- ^b Small Animal Referral Center, Kleintierzentrum am Schmelzbach, Am Schmelzbach 41A, 08112, Wilkau-Haßlau, Germany
- ^c Department of Veterinary Science, University of Turin, Largo Paolo Braccini, 2 10095, Grugliasco, Turin, Italy

Received 21 April 2025; received in revised form 19 July 2025; accepted 22 July 2025

KEYWORDS

Sinotubular junction; Myxoid; Trabecula; Pathology **Abstract** A six-week-old Labrador retriever was presented for lethargy and anorexia, revealing a systolic heart murmur. Tricuspid valve dysplasia involving the whole tricuspid valve apparatus and the right ventricular wall was found, and an additional pulmonic stenosis was present. Histopathological examination of the tricuspid and pulmonary leaflets highlighted an unusual myxomatous mesenchymal component, interpreted as being of ontogenetic origin.

© 2025 The Author(s). Published by Elsevier B.V. This is an open access article under the CC BY license (http://creativecommons.org/licenses/by/4.0/).

Presentation of the case: Online cardiology pathology rounds on the 6th December 2024.

E-mail address: jessica.schoebel@tierdoc-team.de (J. Schoebel).

^{*} A unique aspect of the Journal of Veterinary Cardiology is the emphasis on additional web-based images permitting the detailing of procedures and diagnostics. These images can be viewed (by those readers with subscription access) by going to http://www.sciencedirect.com/science/journal/17602734. The issue to be viewed is clicked and the available PDF and image downloading is available via the Summary Plus link. The supplementary material for a given article appears at the end of the page. Downloading the videos may take several minutes. Readers will require at least Quicktime 7 (available free at http://www.apple.com/quicktime/download/) to enjoy the content. Another means to view the material is to go to https://doi.org/10.1016/j.jvc.2025.07.008.

^{*} Corresponding author.

J. Schoebel et al.

A six-week-old female Labrador retriever was presented due to lethargy, hyporexia, retarded growth, and diarrhea. It was subsequently referred to the cardiology department because of a heart murmur on auscultation. Physical examination revealed a grade 5 holosystolic right apical murmur and a grade 5 holosystolic left basilar murmur, normal pulses, and no cyanosis. An echocardiogram was performed using a Philips d machine with a 12- MHz transducer, and echocardiographic standard views [1] were obtained. Right parasternal long-axis view showed both severe concentric hypertrophy as well as volume overload of the right ventricle (right ventricular end-diastolic area normalized to $kg^{0.665} = 2.48 \text{ cm}^2/kg^{0.665}$ and right ventricular endsystolic area normalized to $kg^{0.695} = 1.61 \text{ cm}^2/kg^{0.695}$ [2]) and left ventricular volume underfilling (left ventricular end-diastolic volume = 1.1 mL and endsystolic volume = 0.3 mL using Simpson's method of discs [3]) with septal flattening and paradoxic motion of the interventricular septum (Video 1). The right atrium was severely dilated with deviation of the interatrial septum toward the left, and tricuspid valve dysplasia was identified. Deformed septal and parietal leaflets of the tricuspid valve with foreshortened, almost absent, chordae tendineae and aberrant attachments were visible. The leaflets overall appeared thickened and hypomotile with reduced diastolic excursion. An intracavitary trabecular structure showing the echogenicity of myocardium as well as an area of hyperechogenicity and a muscular structure compatible with an abnormal papillary muscle were seen. Additional evaluation was accomplished using a left apical fourchamber view (Video 2) and left apical cranial view (Video 3), both optimized for the right ventricle, further confirming the presence of subvalvular trabecular tissue and tethering of the parietal leaflet of the tricuspid valve. The whole tricuspid apparatus and right ventricular inflow tract were concerned (Fig. 1). Functionally, severe tricuspid regurgitation with a maximum regurgitant velocity of 5.34 m/s was present, indicating elevated right ventricular systolic pressure. Additionally, tricuspid valve stenosis was diagnosed using continuous wave Doppler and color flow Doppler (Video 4). Spectral Doppler interrogation of tricuspid inflow showed a mean pressure gradient of 11.3 mmHg, a maximum pressure gradient of 23.5 mmHg, and a pressure half time of 83 ms indicating relevant stenosis [4-6]. A right parasternal heart base view optimized for the main pulmonary artery showed pulmonic stenosis (videos 5-6) with a maximum systolic velocity of 5.18 m/s indicating a severe gradient. Structurally. combined valvular commissural fusion and adhesions at the sinotubular junction with connection to the pulmonic cusps, earlier described as supravalvular stenosis, were detected (Fig. 2). The annulus appeared mildly hypoplastic determined by subjective assessment and a pulmonary-to-aortic ratio of 0.75 being lower than 1, as described by Markovic et al. [7]. Moderate poststenotic dilatation as well as moderate pulmonic valve regurgitation was present. Echocardiographic findings were consistent with dysplasia of the tricuspid and pulmonary valve apparatus. Secondarily, right ventricular concentric hypertrophy combined with volume overload was present and right atrial and auricular dilatation was noted. Following severe right atrial dilatation, with a maximum right atrial diameter of 21.9 mm, assessment of the caudal vena cava and hepatic veins was performed, revealing subjectively distended hepatic veins as well as reduced caudal vena cava collapsibility index of 6.25% [8]. No ascites or pleural effusion was evident at the time of echocardiographic examination. The dog was started on spironolactone and benazepril.

Two weeks later, the dog was presented due to worsening of its clinical condition, showing labored breathing, polypnea, anorexia and a distended undulating abdomen, inappetence, and retarded growth. The owners declined further investigation or therapy, and the dog was euthanized and subsequently sent for pathologic examination. The heart and lungs were examined postmortem. On external examination, there was severe dilatation of the right atrium and right atrial appendage. Also, dilatation of the cranial and caudal vena cava was obvious following congestion. The pulmonary artery did not clearly show dilatation from the external examination, while the right branch appeared more voluminous than the left.

From the atrial view, a transverse muscular trabecula in the middle of the tricuspid ostium between the septal leaflet and the space between the angular leaflet and the right ventricular wall was observed [Fig. 3(A)]. The tricuspid apparatus showed severe malformation with a rounded shape of the three thickened and deformed leaflets and shortened, almost absent, chordae tendineae. The right ventricle and tricuspid apparatus did not reveal normal papillary muscles, but a myocardial trabeculum was found in the cavity just ventral to the tricuspid leaflets between a dysplastic papillary muscle and the interventricular septum. An additional finding was an abnormal wall of the right ventricle with multifocal muscular trabecular structures [Fig. 3(B)].

^d EPIQ 7, Philips GmbH Market DACH, Hamburg, Germany.

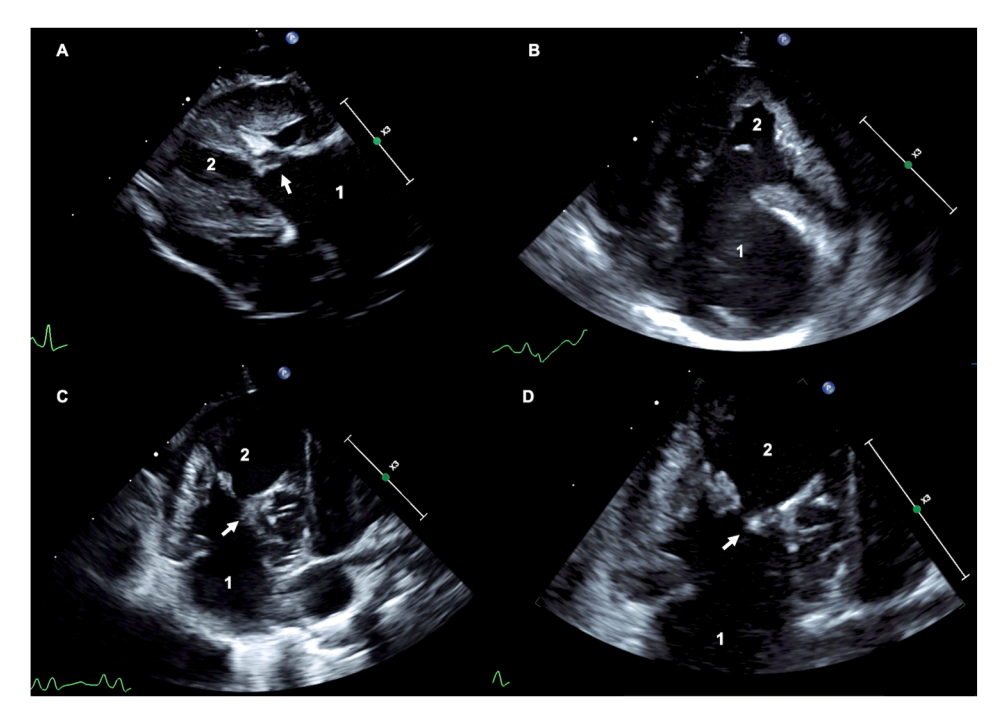


Figure 1 Right parasternal long-axis view (A), left apical cranial view optimized for the right ventricle (B), and left apical four-chamber view optimized for the right ventricle (C) with a close-up of the tricuspid valve apparatus (D) showing severe tricuspid dysplasia with the presence of subvalvular trabecular tissue (arrow) and tethering of the parietal leaflet of the tricuspid valve. Numbers 1 and 2 label the right atrium and right ventricle, respectively.

A longitudinal cut section of the pulmonary artery and valve showed a prominent folding of the wall inducing narrowing of the sinotubular junction. Additionally, the valvular cusps were thickened, irregular, and fused with the endothelium of the dorsal portion of the sinuses of Valsalva [Fig. 4(A)].

Histology of the tricuspid valve showed myxomatous tissue that occupied the entire extension of the flaps [Fig. 3(C)]. Histology of the pulmonic valve and the first portion of the pulmonary artery highlighted a folding of the wall at the sinotubular junction with consequent reduction of the cavity. The cusps also showed fusion with the endothelium of the dorsal area of the sinuses of Valsalva and widespread thickening caused by myxomatous tissue [Fig. 4(B)].

Pathologic diagnosis based on gross and histological examination is consistent with severe dysplasia of the tricuspid valve apparatus as well as valvular pulmonic stenosis with evidence of diffuse myxomatous tissue in the cusps of both valves.

Discussion

Tricuspid dysplasia in canine individuals covers a spectrum of abnormalities leading to functional insufficiency and/or stenosis of the tricuspid valve

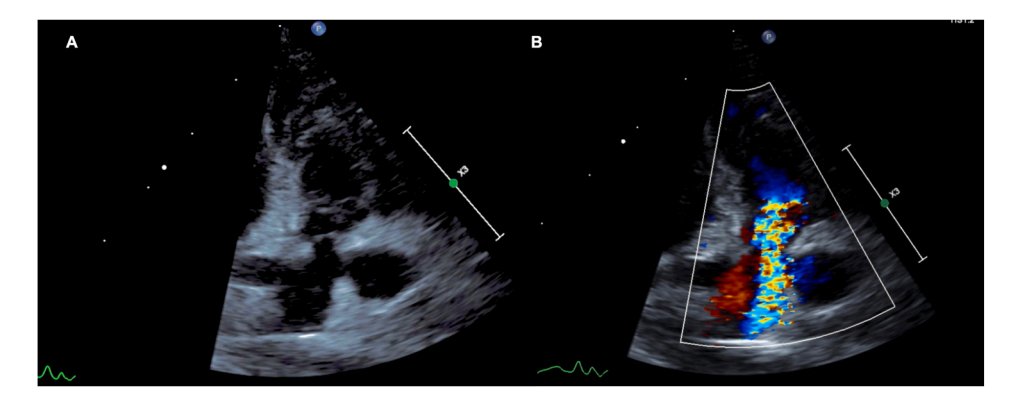


Figure 2 Main pulmonary artery displaying mild annular hypoplasia and stenosis of the pulmonic valve with fusion of the leaflets, as well as adhesions at the sinotubular junction (A), further visualized by color flow Doppler (B).

48 J. Schoebel et al.

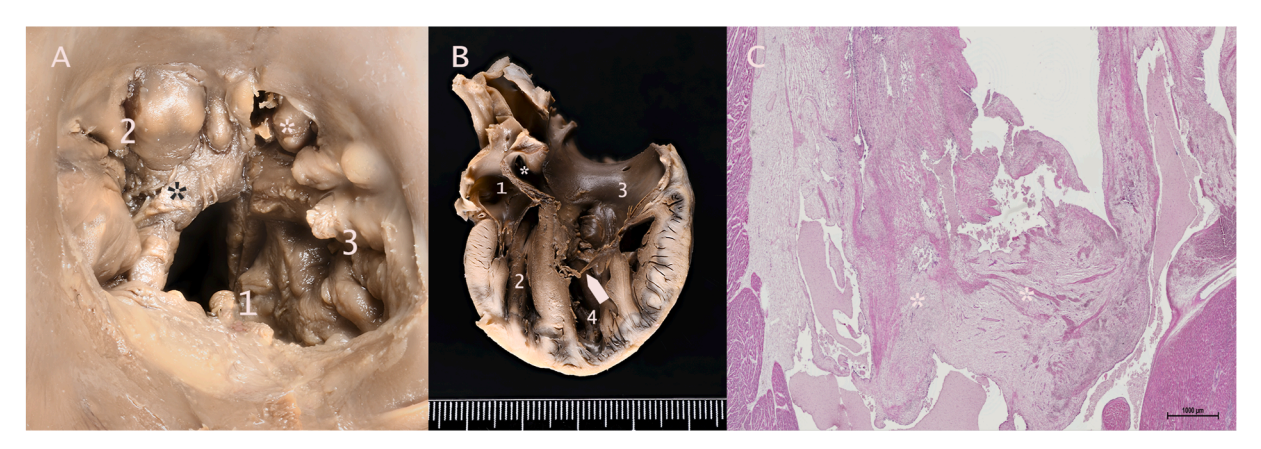


Figure 3 (A) Tricuspid valve seen from the atrial side. The three particularly rounded and deformed cusps can be observed. The asterisk indicates a muscular trabecula that passes through the ostium just ventral to the angular leaflet. 1: Septal leaflet. 2: Angular leaflet. 3: Parietal leaflet. *: Leaflet breakage occurred during manipulation and dissection of the heart. (B) Longitudinal section of the heart with exposure of the four chambers. The tricuspid valve has thickened and deformed leaflets and hypoplastic chordae tendineae. Immediately ventral to the leaflets, the muscular trabecula can be appreciated that crosses the ostium (arrow). Note the anomalous conformation and severe hypertrophy of the papillary muscle and the trabecular structure of the right ventricle wall. 1: Left atrium. 2: Left ventricle. 3: Right atrium. 4: Right ventricle. Asterisk: Interatrial septum, note the deformation caused by its movement toward the left atrium. (C) Histological finding of a tricuspid valve leaflet characterized by severe thickening caused by diffuse myxomatous tissue (*). Hematoxylin and eosin staining.

[9–11]. It is one of the most common congenital heart diseases in Labrador retrievers [10,12,13]. Most commonly, shortened chordae tendineae with direct papillary muscle attachment of the valve and tethering of the septal leaflet leading to tricuspid valve regurgitation are present. Ebstein's anomaly is further described leading to an atrialization of ventricular myocardium and apical displacement of the tricuspid apparatus [14,15]. Less commonly, tricuspid dysplasia involves commissural fusion of the valve with functional stenosis. The

underlying case showed a unique intracavitary trabecular muscular structure connected to the tricuspid apparatus leading to insufficiency and stenosis which differs from the more commonly identified morphotype. A similar finding has been described in humans by Mohan et al. revealing an apical trabeculation leading to right ventricular apical isolation [16]. The pulmonary valve revealed thickening and commissural fusion leading to stenosis and showed additional adhesions at the sinotubular junction, previously only described



Figure 4 (A) Longitudinal cut section of the pulmonary valve at the level of the ostium (*). The arrow indicates the folding of the sinotubular junction with consequent thickening of the wall and reduction of the cavity. Note the severe thickening of the cusps. (B) Histological finding of the pulmonary valve and the first portion of the pulmonary artery showing the folding of the wall at the sinotubular junction (arrow), fusion of the cusps with the endothelium (*), and diffuse thickening caused by myxomatous tissue. Hematoxylin and eosin staining.

using angiography by Scansen et al. [17]. A clear classification into type A characterized by valvular commissural fusion, systolic doming, a normally sized annulus, and poststenotic dilation or type B defined by marked leaflet thickening, pulmonary annulus hypoplasia, and infundibular hypertrophy with rare poststenotic dilation could not be performed as recommended by Bussadori et al. [18]. The presence of features of both types was given. Regarding the folding of the pulmonary sinotubular junction with consequent reduction of the cavity, it remains to be further established whether this localization can be considered valvular or—even if in the very first portions—already supravalvular. Histologically, myxomatous tissue of both valves leading to thickening was present. Following a review of previous publications investigating pulmonic stenosis and tricuspid dysplasia of the entire apparatus, this report presents the first documented case of an ontogenetic manifestation of myxomatous tissue affecting both valves, at the inflow and outflow tracts, of the right heart. However, a human case report described a myxoid and hypercellular lesion of the tricuspid valve with shortened, thickened leaflets [19]. Different assumptions could be made for explanation. First of all, possible shear stress might lead to early remodeling [20] and replacement of normal cells, as discussed in myxomatous mitral valve disease [21-23]. Another possible mechanism might include a congenital maldevelopment and integrity of cells of mesenchymal origin. Pulmonary cusps derive from swellings of subendothelial mesenchymal tissue, and remodeling leads to formation of the thin cusp structure. Atrioventricular valves partially derive from mesenchymal tissue. During fetal development, mesenchymal tissue grows around the rim of the valve orifice, and cavitation of the muscular layer and remodeling of the tissue contribute to cusp formation [24]. Failure in this cavitation and remodeling process might lead to maldevelopment. Altered gene regulation is additionally discussed to be a contributor to atrioventricular valve dysplasia and altereccellular tissue [25].

A further unusual auxiliary finding was hypertrophied and very prominent pectinate muscles, even though the right auricle generally encorporates more extensive pectinate muscles than the left one. Loukas et al. described different types of pectinate muscles in humans [26]. Based on this classification, type VI might be the most applicable type in our case. It is characterized by a prominent muscular column with velamentous pectinate muscles. As right atrial dilatation might have already been present shortly after birth, early remodeling with hypertrophy of the pectinate muscles instead of predominant atrial and auricular wall dilatation might have occurred [27].

Conclusion

A myxomatous lesion following severe dysplasia of the tricuspid valve apparatus involving the right ventricular wall and pulmonary stenosis consisting of valvular stenosis and stenotic tissue at the level of the sinotubular junction has been diagnosed. Following review of previous publications, this report presents the first documented case of an ontogenetic manifestation of myxomatous tissue affecting two valves including the entire apparatus.

Declaration of Competing Interest

The authors do not have any conflicts of interest to disclose.

Supplementary data

Supplementary data related to this article can be found at https://doi.org/10.1016/j.jvc. 2025.07.008.

Video Two-dimensional image of a right parasternal long axis

1 view overload and flattening of the interventricular septum as well as left ventricular volume underfilling can be detected. Furthermore, an area of hyperechogenicity attached to the dysplastic tricuspid valve apparatus is visible.

50 J. Schoebel et al.

Video 2	Two-dimensional image of a left apical four-chamber view optimized for the right ventricle	Dysplasia of the tricuspid valve with subvalvular trabeculation is demonstrated with involvement of the whole tricuspid valve apparatus.
Video 3	Two- dimensional image of a left apical cranial view optimized for the right ventricle	Reduced excursion and tethering of a tricuspid leaflet is demonstrated.
Video 4	Left apical four-chamber view optimized for the right ventricle with colour flow doppler over the tricuspid valve apparatus	Evidence of a diastolic candle flame sign can be appreciated following tricuspid valve stenosis and significant tricuspid valve regurgitation can be detected during systole.
Video 5	Two-dimensional image of a right apical heart base view optimized for the pulmonary artery	Pulmomic stenosis wih annular hypoplasia and essentially reduced motility of the pulmonic cusps as well as adhesions at the sinotubular junction are visualized.
Video 6	Right apical heart base view optimized for the pulmonary artery with colour flow doppler over the pulmonic valve	Systolic turbulance secondary to flow acceleration over the pulmonic stenosis and pulmonic regurgitation during diastole are shown.

References

- [1] Thomas WP, Gaber CE, Jacobs GJ, Kaplan PM, Lombard CW, Moise NS, Moses BL. Recommendations for standards in transthoracic two-dimensional echocardiography in the dog and cat. Echocardiography Committee of the Specialty of Cardiology, American College of Veterinary Internal Medicine. J Vet Intern Med. 1993;7(4): 247-52.
- [2] Feldhütter EK, Domenech O, Vezzosi T, Tognetti R, Sauter N, Bauer A, Eberhard J, Friederich J, Wess G. Echocardiographic reference intervals for right ventricular indices, including 3-dimensional volume and 2-dimensional strain measurements in healthy dogs. J Vet Intern Med. 2022;36(1):8–19.
- [3] Wess G, Bauer A, Kopp A. Echocardiographic reference intervals for volumetric measurements of the left ventricle using the Simpson's method of discs in 1331 dogs. J Vet Intern Med. 2021;35(2):724–38.
- [4] Stamm RB, Martin RP. Quantification of pressure gradients across stenotic valves by Doppler ultrasound. J Am Coll Cardiol. 1983;2(4):707–18.
- [5] Lehmkuhl LB, Ware WA, Bonagura JD. Mitral stenosis in 15 dogs. J Vet Intern Med. 1994;8(1):2—17.
- [6] Oyama MA, Weidman JA, Cole SG. Calculation of pressure half-time. J Vet Cardiol. 2008;10(1):57–60.
- [7] Markovic LE, Scansen BA, Hiremath G, Kellihan HB, Tjostheim SS, Calkins C, Hodges KM, Cahill E, Tainter B, Carter M, Kim DW. Comparative transcatheter intervention for pulmonary valve stenosis: multicenter collaborative study across pediatric and veterinary cardiology centers. J Vet Cardiol. 2025;58:26—37.
- [8] Chou YY, Ward JL, Barron LZ, Murphy SD, Tropf MA, Lisciandro GR, Yuan L, Mochel JP, DeFrancesco TC. Focused ultrasound of the caudal vena cava in dogs with cavitary effusions or congestive heart failure: a prospective, observational study. PLoS One. 2021;16(5): e0252544.
- [9] Bussadori C. Tricuspid dysplasia. In: Bussadori C, editor. Textbook of Cardiovascular Medicine in Dogs and Cats. Edra Publishing; 2023. p. 395—421.
- [10] Navarro-Cubas X, Palermo V, French A, Sanchis-Mora S, Culshaw G. Tricuspid valve dysplasia: a retrospective study

- of clinical features and outcome in dogs in the UK. Open Vet J. 2017;7(4):349–59.
- [11] Sousa M, Gerardi D, Alves R, Camacho A. Tricuspid valve dysplasia and Ebstein's anomaly in dogs: case report. Arquivo Brasileiro De Medicina Veterinaria E Zootecnia -ARQ BRAS MED VET ZOOTEC. 2006;58.
- [12] Brambilla PG, Polli M, Pradelli D, Papa M, Rizzi R, Bagardi M, Bussadori C. Epidemiological study of congenital heart diseases in dogs: Prevalence, popularity, and volatility throughout twenty years of clinical practice. PLoS One. 2020;15(7):e0230160.
- [13] Chetboul V, Tran D, Carlos C, Tessier D, Pouchelon JL. [Congenital malformations of the tricuspid valve in domestic carnivores: a retrospective study of 50 cases]. Schweiz Arch Tierheilkd. 2004;146(6):265—75.
- [14] Andelfinger G, Wright KN, Lee HS, Siemens LM, Benson DW. Canine tricuspid valve malformation, a model of human Ebstein anomaly, maps to dog chromosome 9. J Med Genet. 2003;40(5):320–4.
- [15] Chetboul V, Poissonnier C, Bomassi E, Jamin C, Pouchelon JL, Tissier R, Desquilbet L. Epidemiological, clinical, and echocardiographic features, and outcome of dogs with Ebstein's anomaly: 32 cases (2002-2016). J Vet Cardiol. 2020;29:11–21.
- [16] Mohan J, Shukla M, Mohan V, Sethi A. Congenitally unguarded tricuspid valve orifice with right ventricular apical isolation in an adult. Indian Heart J. 2015;68.
- [17] Scansen BA. Cardiac Interventions in small animals: areas of uncertainty. Vet Clin North Am Small Anim Pract. 2018; 48(5):797—817.
- [18] Bussadori C, DeMadron E, Santilli RA, Borgarelli M. Balloon valvuloplasty in 30 dogs with pulmonic stenosis: effect of valve morphology and annular size on initial and 1-year outcome. J Vet Intern Med. 2001;15(6):553—8.
- [19] Litovsky SH, Kelly DR, Law MA, Dabal RJ, Daniel RL, Cleveland DS, Pearce FB. Shone variant with large eustachian valve: implication for repair and heart transplantation. Cardiovasc Pathol. 2015;24(2):124–7.
- [20] Rabkin-Aikawa E, Farber M, Aikawa M, Schoen FJ. Dynamic and reversible changes of interstitial cell phenotype during remodeling of cardiac valves. J Heart Valve Dis. 2004;13 (5):841—7.

- [21] Rabkin E, Aikawa M, Stone JR, Fukumoto Y, Libby P, Schoen FJ. Activated interstitial myofibroblasts express catabolic enzymes and mediate matrix remodeling in myxomatous heart valves. Circulation. 2001;104(21): 2525–32.
- [22] Togashi M, Tamura K, Nitta T, Ishizaki M, Sugisaki Y, Fukuda Y. Role of matrix metalloproteinases and their tissue inhibitor of metalloproteinases in myxomatous change of cardiac floppy valves. Pathol Int. 2007;57(5): 251–9.
- [23] Kim TS, Hong CY, Oh SJ, Choe YH, Hwang TS, Kim J, Lee SL, Yoon H, Bok EY, Cho AR, Do YJ, Kim E. RNA sequencing provides novel insights into the pathogenesis of naturally occurring myxomatous mitral valve disease stage B1 in beagle dogs. PLoS One. 2024;19(5):e0300813.
- [24] Cardiovascular system. In: Kilroy D, Quinn PJ, McGeady T, Ryan M, Fitzpatrick E, Lonergan P, editors. Veterinary Embryology. 2nd ed. John Wiley & Sons; 2017. p. 119–47.
- [25] Yan S, Peng Y, Lu J, Shakil S, Shi Y, Crossman DK, Johnson WH, Liu S, Rokosh DG, Lincoln J, Wang Q, Jiao K. Differential requirement for DICER1 activity during the development of mitral and tricuspid valves. J Cell Sci. 2022;135(17).
- [26] Loukas M, Tubbs RS, Tongson JM, Polepalli S, Curry B, Jordan R, Wagner T. The clinical anatomy of the crista terminalis, pectinate muscles and the teniae sagittalis. Ann Anat. 2008:190(1):81—7.
- [27] Neradilova C, Gregorovicova M, Kovanda J, Kvasilova A, Melenovsky V, Nanka O, Sedmera D. "Form follows function": the developmental morphology of the cardiac atria. Physiol Res. 2024;73(S3):S697—s714.

Available online at www.sciencedirect.com

ScienceDirect